

Effects of Silica and Titania Supports on the Catalytic Performance of Vanadium-Phosphorus-Oxide Catalysts[#]

M. Ruitenbeek^{*}, A.J. van Dillen, D.C. Koningsberger, and J. W. Geus

Utrecht University, Debye Institute, Department of Inorganic Chemistry,
PO Box 80.083, 3508 TB, Utrecht, The Netherlands

Silica - and titania-supported V-P-O catalysts (~8 wt.% V) were prepared by means of homo-geneous deposition precipitation and compared with an 'organic' bulk V-P-O catalyst. All samples were tested in the selective oxidation of *n*-butane to maleic anhydride (MA), and characterised with X-ray absorption spectroscopy (EXAFS).

The catalytic performance of VPO/TiO₂ on the one hand and VPO/SiO₂ and VPO/bulk on the other hand is remarkably different. EXAFS data analysis revealed that these differences can be explained by structural differences between the V-P-O phases in the different catalysts. However,

VPO/SiO₂ and VPO/bulk, which display comparable yields to MA, show a different EXAFS spectrum. This indicates that the active phase in this reaction is not vanadylpyrophosphate.

1. INTRODUCTION

Catalysts based on Vanadium-Phosphorus-Oxide (V-P-O) are industrially used for the production of maleic anhydride (MA) from *n*-butane. The V-P-O system has been under investigation for the last three decades, and although it is widely accepted that vanadylpyrophosphate, (VO)₂P₂O₇, is the main component in the active catalyst, still little is known about the exact nature of the catalytic active site (1-3).

At Utrecht University much effort is devoted to the development of supported V-P-O catalysts (4-6). It can be expected that the supported V-P-O catalysts have superior characteristics over bulk V-P-O, such as a cheap and reproducible preparation procedure, a large active surface area, a short activation period and a high mechanical strength. Therefore, application of supported V-P-O catalysts in a fluidised-bed process could be very promising. Our newly developed catalysts show interesting catalytic properties. For instance titania-supported V-P-O is already active at low temperatures (250°C), although the selectivity is low

[#] Netherlands Institute for Research in Catalysis (NIOK) publication # UU 98-1-04 and UU 98-2-01

^{*} Corresponding author, e-mail: m.ruitenbeek@chem.ruu.nl

(4,6). Silica-supported V-P-O catalysts, on the other hand, show reasonable yields in maleic anhydride (5), and these systems are being further optimised in our laboratory.

In literature, only a few other examples of deposition of V-P-O on silica (7,8), titania (9), alumina (9-12) and AlPO_4 (13) have been described. In general, with supported V-P-O catalysts, the lack of long-range order of the supported V-P-O particles makes a proper characterisation of the supported V-P-O phase with common techniques like X-ray diffraction or FTIR spectroscopy difficult or even impossible. Nevertheless, most supported V-P-O catalysts are reported to consist of a phase that strongly resembles V^{5+} -phosphate, mostly γ - VOPO_4 (14,15).

Generally, the catalytic activity of the V-P-O catalysts has been related to the local structure of surface vanadyl groups in vanadylpyrophosphate. However, with most techniques, no explicit information about this active surface is obtained. The structure of crystalline vanadylpyrophosphate consists of pairs of edge-sharing pseudo octahedral co-ordinated vanadium ions at a distance of 3.23 Å, isolated from other pairs by pyrophosphate groups (16). This structural unit is often used to model the active sites in V-P-O catalysts (2,17,18). Moreover, in the literature, various other models have been proposed, *i.e.* interfaces between different VOPO_4 phases and $(\text{VO})_2\text{P}_2\text{O}_7$ (14,15), V^{5+} sites on the surface of $(\text{VO})_2\text{P}_2\text{O}_7$ (2), V^{5+} species in interaction with $\text{VO}(\text{PO}_3)_2$ (19), and amorphous V^{4+} and/or V^{5+} phases supported on crystalline $(\text{VO})_2\text{P}_2\text{O}_7$ (20,21).

In this paper we have studied the structure-activity relationship of our supported V-P-O catalysts. To this end we have applied catalytic measurements and X-ray absorption spectroscopy (EXAFS). For this technique crystallinity of the samples is not a prerequisite.

2. EXPERIMENTAL

2.1. Catalyst preparation

The catalysts used for this study were bulk V-P-O, titania-supported V-P-O (8.2 wt.% V), and silica-supported V-P-O (7.5 wt.% V). All catalysts were prepared with a P/V ratio of 1.1. Bulk V-P-O was prepared in *i*-butanol according to a well known procedure (22). This catalysts will be denoted VPO/bulk.

Supported V-P-O catalysts have been prepared on TiO_2 (Degussa P25) and SiO_2 (Engelhard C500-20) according a procedure described by Overbeek *et al.* (4,5). This method is based on homogeneous precipitation (HDP) of V(III) species in the presence of $\text{NH}_4\text{H}_2\text{PO}_4$. To this end V^{V} was electrochemical reduced first to V^{III} ions in diluted hydrochloric acid solution.

In a typical experiment 10 grams of the support material was suspended in 1500 ml demineralised water and stirred vigorously. Secondly, the pH of the solution was decreased by addition of concentrated hydrochloric acid (pH~2). Next, an appropriate amount of V(III) electrolyte was added, followed by $\text{NH}_4\text{H}_2\text{PO}_4$ (P/V ratio 1.1). The pH was homogeneously increased by addition of a 5 wt.% ammonia solution at a rate of ~0.1 mmol OH^- per minute. Addition was stopped at pH~7. The suspension was filtered and dried (air, 120°C, 16 hours).

For the preparation of silica-supported catalysts this method was slightly adapted, because of the poor interaction of the V-P-O with silica (5,23). First an amount of vanadium oxide was

precipitated, which was subsequently impregnated with diluted phosphoric acid to obtain silica-supported V-P-O. The supported catalysts will be referred to as VPO/TiO₂ and VPO/SiO₂ respectively.

Finally, catalyst precursors were calcined in N₂ at 450°C for 16 h prior to testing and characterisation.

2.2. Catalyst performance testing

After calcination, both bulk and supported V-P-O catalysts were tested in the selective oxidation of *n*-butane using a 1.5% *n*-butane, 20.5% O₂, 78.5% Ar flow (1.5 ml catalyst, 50 ml/min, GHSV=2000 h⁻¹) at atmospheric pressure. Formed gaseous products, as well as unconverted reactants were analysed using an on-line Balzers QMA-420 mass spectrometer operating at 150 °C to avoid condensation of products. Carbon mass balances were in the range of 0.98 to 1.02. A detailed description of the experimental conditions is given in earlier publications (4,5).

2.3. Catalyst characterisation

All catalysts have been characterised with X-ray absorption spectroscopy (XANES/EXAFS). EXAFS data were collected at Station 8.1 of the SRS facility in Daresbury (UK). The energy of the electron beam amounted to 2 GeV (average current ~ 150 mA). The Si [111] double crystal was detuned to 70 % intensity to minimise the presence of higher harmonics. The measurements were all carried out in transmission mode using optimised ionisation chambers as detectors. To minimise noise the counting time per data point was taken 1000 ms, and at least three scans were recorded and averaged. All samples were recorded *ex-situ* in He at -196°C after calcination of the fresh precursor in nitrogen at 450°C for 16 h. The energy calibration was performed by means of a V-foil (5µm). The absolute value of the vanadium-edge is 5465 eV.

The catalyst samples were pressed into self-supporting wafers and mounted in an in-situ EXAFS cell (24). The thickness of the wafer was chosen in such a way as to give an absorbance (µx) of 2.5 for optimal signal-to-noise ratio. To prevent self-absorption by the catalysts the amount of sample was chosen to obtain a step in absorbance of 1.0 in the edge region (Δµx=1). If necessary, samples were diluted with boron nitride (BN). Standard procedures were used to extract the EXAFS data from the measured absorption spectrum. The background was subtracted using cubic spline routines (25). Normalisation was done by dividing the data by the height of the absorption at 50 eV.

3. RESULTS AND DISCUSSION

3.1. Catalyst Performance Testing

In Figure 1 the conversion as a function of temperature of VPO/bulk, VPO/TiO₂ and VPO/SiO₂ are represented. It is obvious that VPO/TiO₂ is the most active catalyst, showing conversion at 250°C already. In general, our titania-supported catalysts are even more active at lower loadings (4). Despite the lower amount of V-P-O present in the silica-supported catalyst,

this sample is more active than the bulk catalyst. This difference can be explained by the higher specific surface area of the active component in the supported catalysts.

Both VPO/bulk and VPO/SiO₂ show about the same selectivity to maleic anhydride (Figure 2). However, for VPO/SiO₂ the selectivity decreases much more when the conversion is raised. The selectivity of VPO/TiO₂ at low conversions is substantially below that of the other catalysts and only a yield of 6% is obtained at a conversion of 30%. The differences in activity and selectivity between VPO/TiO₂ on the one hand and VPO/SiO₂ and VPO/bulk on the other hand have been explained by the strong interaction between V-P-O and titania (4,6). Therefore we will focus on the structural characterisation of the samples in the remaining part of this paper.

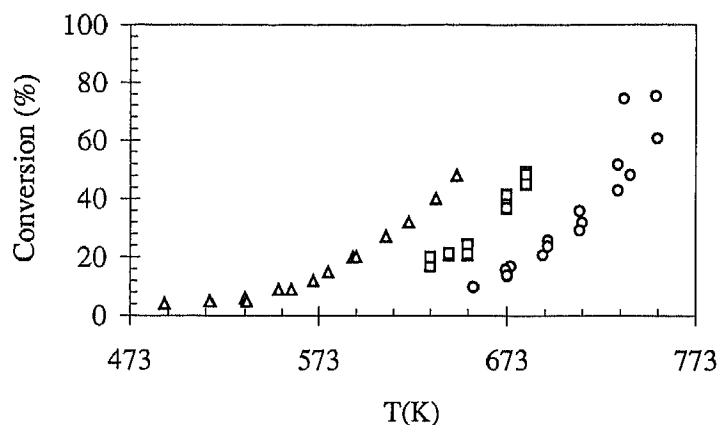


Figure 1. Conversion as a function of temperature for VPO/Bulk (circles), VPO/SiO₂ (squares) and VPO/TiO₂ (triangles). Data were collected in a *n*-butane/oxygen/argon flow (1.5/10/78.5) of 50 ml/min at atmospheric pressure.

3.2. EXAFS

In Figure 3 the k^2 Fourier Transform of VPO/bulk and VPO/SiO₂ is shown ($0.5\text{\AA} < R < 4.5\text{\AA}$, no phase correction). It is obvious that the imaginary parts of the two Fourier transform differs significantly around 1.5\AA . This is the range where the contributions of the first-shell oxygen atoms are located. Furthermore, an important extra contribution at $\pm 2\text{\AA}$ is present in the data of VPO/TiO₂. For the higher co-ordination shells the spectra of bulk and supported V-P-O differ considerably. A detailed description of the EXAFS data analysis of both bulk and supported V-P-O catalysts will be published elsewhere (26).

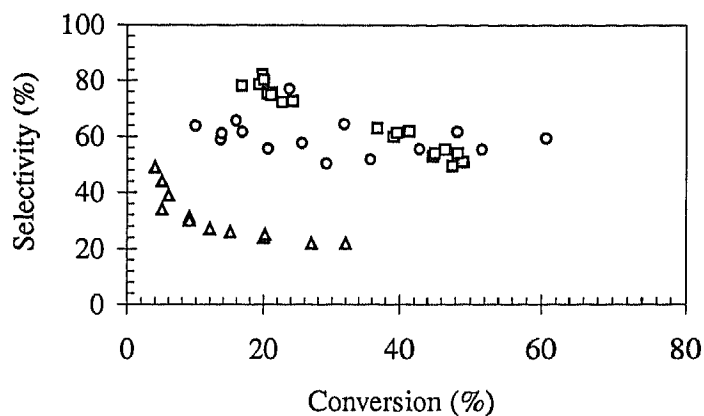


Figure 2. Selectivity as a function of conversion for VPO/bulk (circles), VPO/SiO₂ (squares) and VPO/TiO₂ (triangles)

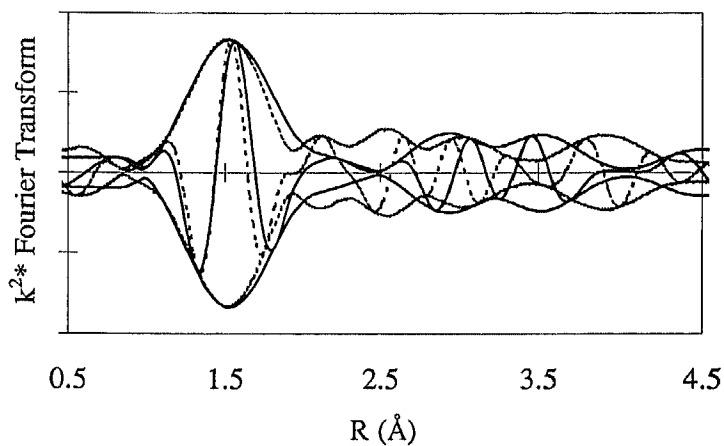


Figure 3. $0.5 < R < 4.5 \text{ \AA}$ range of the k^2 Fourier Transform of the EXAFS data of VPO/bulk (solid line) and VPO/SiO₂ (dotted line).

Recently, Nguyen *et al.* have revealed the structure of crystalline vanadylpyrophosphate (16). Our EXAFS data of VPO/bulk could be fit up to a distance of 3.5 Å with the single crystal X-ray data of Nguyen *et al.* (16). Above this threshold too many contributions must be included in

the calculations. This results in a low reliability of the final fit. The results of the EXAFS data analysis of VPO/bulk have been published elsewhere (27).

Although an appreciable amount ($\pm 30\%$) of our VPO/bulk consists of an amorphous V-P-O phase (28), the EXAFS spectrum is dominated by the structure of the ideal vanadylpyrophosphate structure. This is the major constraint for the application of techniques like XRD or EXAFS to study active bulk V-P-O catalysts.

Figure 4 represents the k^2 Fourier transforms of the EXAFS data of both supported catalysts. Again these spectra are totally different for both the first co-ordination shell and for the higher shells. It is important to note that the spectrum of VPO/TiO₂ also deviates from that of VPO/bulk.

As stated above EXAFS is a bulk technique. Since the EXAFS spectrum of VPO/SiO₂ is not suffering from interfering dominant bulk contributions, we think that the EXAFS spectrum of VPO/SiO₂ represents the structure of the surface phase that is present in VPO/bulk.

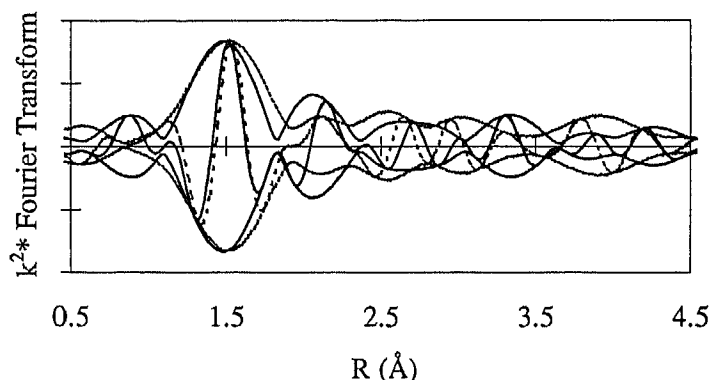


Figure 4. $0.5 < R < 4.5 \text{ \AA}$ range of the k^2 Fourier Transform of the EXAFS data of VPO/SiO₂ (dotted line) and VPO/TiO₂ (solid line).

Although we have not finished data analysis yet, but the first results indicate that VPO/TiO₂ consists of small particles in which the V atoms are tetrahedrally co-ordinated by other oxygen atoms, including V-O-Ti oxygen atoms. The VPO/SiO₂ catalyst on the other hand consists of vanadyl groups in an octahedral environment. It is important to note that with both supported V-P-O catalysts no V-V contributions were found in the EXAFS data up to a distance of 3.5 Å.

4. CONCLUSIONS

Supported V-P-O catalysts have been tested in the *n*-butane oxidation reaction to maleic anhydride, and characterised with X-ray absorption spectroscopy. Our results indicate that the differences in catalytic performance between VPO/TiO₂ and VPO/SiO₂ can not only be explained by the difference interaction between V-P-O and the respective supports. The combination of characterisation methods has revealed that the structure of the supported V-P-

O phase does not match crystalline vanadylpyrophosphate. Furthermore there are large differences between the structures of the supported compounds.

Since VPO/SiO₂ is exhibiting a yield close to the yield of our bulk catalyst we think that the oxidation of *n*-butane to maleic anhydride takes place over an (amorphous) surface V-P-O phase. Therefore it will be interesting to study the structure of the VPO/SiO₂ catalyst in more detail, and with different techniques. A detailed analysis of the EXAFS data of the silica-supported V-P-O catalyst (26) can give more insight in the nature of the real active site of the maleic anhydride catalyst.

REFERENCES

1. B.K. Hodnett, *Catal. Rev. -Sci. Eng.* 27(3) (1985), 373
2. G. Centi, F. Trifirò, J.R. Ebner, and V.M. Franchetti, *Chem. Rev.* 88 (1988), 55
3. G. Centi, *Catal. Today* 16, (1993), 5
4. R.A. Overbeek, P.A. Warringa, M.J.D. Crombag, L.M. Visser, A.J. van Dillen, J.W. Geus, *Applied Catalysis A: General* 135 (1996), 209
5. R.A. Overbeek, A.R.C.J. Pekelharing, A.J. van Dillen, J.W. Geus, *Applied Catalysis A: General* 135 (1996), 231
6. M. Ruitenbeek, R.A. Overbeek, A.J. van Dillen, D.C. Koningsberger, J.W. Geus, *Recl. Trav. Chim. Pays-Bas* 115 (1996), 519
7. V.A. Zazhigalov, Yu. P. Zaitsev, V.M. Belousov, B. parlitz, W. Hanke, G. Ohlman, *React. Kinet. Catal. Lett.* 32 (1986), 209
8. K.E. Birkeland, S.M. Babitz, G. K. Bethke, H.H. Kung, G.W. Coulston, S.R. Bare, *J. Phys. Chem. B* 101 (1997), 6895
9. M. Martinez-Lara, L. Moreno-Real, R. Pozas-Tormo, A. Jiminez-Lopez, S. Bruque, P. Ruiz, G. Poncelet, *Can. J. Chem* 70 (1992), 5
10. M. Nakamura, K. Kawai, Y. Fujiwara, *J. Catal.* 34 (1974), 345
11. N.T. Do, M. Baerns, *Appl. Catal.* 45 (1988), 1
12. A. Ramstetter, M. Bearn, *J. Catal* 109 (1988), 303
13. P.S. Kuo, B.L. Yang, *J. Catal.* 117 (1989), 301
14. E. Bordes, *Catal. Today* 1 (1987), 499
15. G.J. Hutchings, A Desmartin-Chomel, R. Olier, J.C. Volta, *Nature* 368 (1994), 41
16. P.T. Nguyen, R.D. Hoffman, and A.W. Sleight, *Mater. Res. Bull.* 30 (1995), 1055
17. P.A. Agaskar, L. DeCaul, R.K. Graselli, *Catal. Lett.* 23 (1994), 339
18. B. Schiott, K.A. Jorgensen, *Catal. Today* 16 (1993), 79
19. M.T. Sananes, A. Tuel, J.C. Volta, *J. Catal.* 145 (1994), 251
20. N. Harrouch Batis, H. Batis, A. Ghorbel, J.C. Vadrine, J.C. Volta, *J. Catal.* 128 (1991), 248
21. G. Bergeret, M. David, J.P. Broyer, J.C. Volta, G. Hecquet, *Catal. Today* 1 (1987), 37
22. K. Katsumoto, D.M. Marquis, US Patent 4,132,670 (1970)
23. R.A. Overbeek, E.J. Bosma, D.W.H. de Blauw, A.J. van Dillen, H.G. Bruil, J.W. Geus, *Applied Catalysis* 163 (1997), 129

24. M. Vaarkamp, B.L. Mojet, J.T. Miller, D.C. Koningsberger, *J. Phys. Chem.* 99 (1995), 16067
25. J.B.A.D. van Zon, D.C. Koningsberger, H.F.J. van Blik, D.E.J. Sayers, *J. Chem. Phys.* 82 (1985), 5742
26. M. Ruitenbeek, A.J. van Dillen, J.W. Geus, D.C. Koningsberger, *to be published*
27. M. Ruitenbeek, R.A. Overbeek, D.C. Koningsberger, J.W. Geus, in *Catalytic Activation and Functionalisation of Light Alkanes*, E.G. Derouane *et al.* (eds.), Kluwer Academic Publishers, Dordrecht (1998), 423
28. M. Ruitenbeek, A. Barbon, E.E. van Faassen, J.W. Geus, *submitted to Catalysis Letters*